ISSN 1054-660X, Laser Physics, 2008, Vol. 18, No. 7, pp. 914–919.

Experimental Investigation of a Passively Mode-Locked Fiber Laser Based on a Symmetrical NOLM with a Highly Twisted Low-Birefringence Fiber

B. Ibarra-Escamilla[a], *, O. Pottiez[b], E. A. Kuzin[a], R. Grajales-Coutiño[a], and J. W. Haus[c]

[a] *Instituto Nacional de Astrofisica, Optica y Electronica, Optics Department, Apdo. Postal 51 y 216, Puebla, Pue 72000, Mexico*

[b] *Centro de Investigaciones en Optica, Leon, Gto 37150, Mexico*

[c] *Electrooptics Program, University of Dayton, Dayton, OH 45469, USA*

*e-mail: baldemar@inaoep.mx

Received February 5, 2008

Abstract—We experimentally investigate the passive mode-locking operation of a figure eight-fiber laser based on a symmetrical nonlinear optical loop mirror (NOLM) with a highly twisted low-birefringence fiber in the loop. NOLM switching is achieved by the polarization asymmetry between the counterpropagating beams in the loop. The most efficient switching is obtained when we have linear polarization for one of the beams and the circular polarization for the other. We used a quarter-wave retarder (QWR) in the NOLM loop to break the polarization symmetry. Through the QWR position, it is possible to adjust the transmission behavior from a maximum to a minimum at a low input power. With our configuration, it is possible to get self-starting mode-locking operation at a specific position of the QWR. This QWR position corresponds to a value close to the minimal transmission. The pulse repetition frequency was 0.8 MHz. The mode-locked laser ran in a stable operation for hours. We achieved a stable generation of picosecond pulses with milliwatts of an average output power.

PACS numbers: 42.81.-i, 42.55.Wd, 42.65.-k

DOI: 10.1134/S1054660X08070177

1. INTRODUCTION

Passive mode locking of lasers requires nonlinear elements for which the transmission grows with the light intensity. A variety of all-fiber configurations was suggested for this aim including a nonlinear optical loop mirror (NOLM) [1] (called figure-eight lasers, F8L) and a nonlinear amplifier loop mirror (NALM) [2]. These configurations were intensively investigated for mode locking [3–5]. The NOLM usually is formed by an asymmetrical coupler whose output ports are connected to form a loop [6]. The power imbalance between the counterpropagating beams results in a difference in the nonlinear phase shift of these beams caused by the self-phase modulation [7]. This, in turn, results in an intensity-dependent transmission of the NOLM required for the passive mode locking. In that case, the polarization of the beams does not contribute to the switching. If we now use a symmetrical coupler in the loop, the switching can be obtained through the dependence of the phase shift on the polarization. Thus, it is then necessary to create a polarization asymmetry between the counterpropagating beams to get the switching. In our previous investigations, we suggested using the NOLM with a symmetrical coupler and the highly twisted fiber in the loop [8, 9]. Extensive theoretical and experimental studies have shown that this scheme allows for a stable operation and provides a simple way to adjust the nonlinear characteristics [10–13]. A high twist reduces the fiber-residual linear birefringence and makes it more robust to changes in the environmental conditions. It was also shown that the twisted fiber has the nonlinear properties equivalent to that of the ideal fiber [14]. Recently, we have demonstrated the passive mode locking using the symmetrical NOLM with a highly twisted fiber and a QWR in the loop [15, 16]. However, the F8L demonstrated in this work was not self-starting and the pulses had a high pedestal. The difficulties of the self-starting operation are well known problems for all-fiber lasers. The self-starting pulsed operation of a passively mode-locked laser occurs when a certain threshold value of the intracavity power is reached [17–19]. There are several papers reporting on the self-starting using a passively mode-locked fiber-ring configuration [20–26]. For the best of our knowledge, the self-starting passive mode-locking operation of an F8L including a NOLM has not yet been reported (it was reported but using a NALM [2]).

In this work, we investigate the details of the operation of an F8L based on a power-balanced NOLM with a twisted low-birefringence fiber and a QWR in the loop. The laser cavity also includes the fiber-Bragg grating filter to generate pulses of picoseconds duration. We used the flexibility of the nonlinear characteristics of the NOLM to find the self-starting operation.

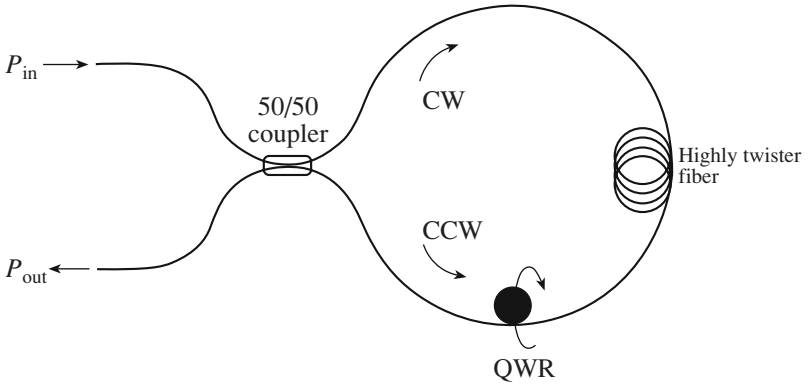

Fig. 1. Schematic diagram of the NOLM. The CW and CCW are the clockwise and counterclockwise directions, respectively. P_{in} and P_{out} are the NOLM input and output power, respectively.

We achieved a stable generation of 30-ps pulses at a repetition frequency of 0.8 MHz with milliwatts of average output power. The self-starting operation was achieved at the specific adjustment of the nonlinear characteristic of the NOLM.

2. THEORY

Figure 1 illustrates the structure of the NOLM used as the switching element. It consists of a symmetrical coupler whose output ports are connected through a highly twisted fiber and a QWR in the loop. The QWR creates a polarization asymmetry between clockwise (CW) and counterclockwise beams into the loop (CCW). The expression of the NOLM transmission is given by [12]

$$T = \frac{1}{2} - \frac{1}{2}\cos\left(\beta - 2\alpha - \frac{1}{4}A_S^{cw}P_{in}l\right) \times \cos\left(\beta - 2\alpha - \frac{1}{4}A_S^{ccw}P_{in}l\right), \quad (1)$$

where β represents the total optical activity of the fiber, α is the QWR angle, P_{in} is the NOLM input power, and l is the normalized fiber length (here $l = L/L_b$, where L is the absolute length (in meters) and L_b is the fiber beat length; $P_{in} = 2P_N$, where $P_N = b\pi P/k$ is the normalized power, P is the power in the fiber and $b = 4\pi c_2/3\lambda A_{eff}$ is the nonlinearity coefficient; c_2 is the Kerr coefficient, λ is the wavelength, and A_{eff} is the effective modal area). Here, A_S^{cw} and A_S^{ccw} are the Stokes parameters for the CW and CCW beams, respectively.

In the case of the circular polarization for the input beam, we will have circular polarization for the CW beam ($A_S^{cw} = 1$) and the linear polarization for the CCW beam ($A_S^{ccw} = 0$). In this case, Eq. (1) is a simple cosine function of P_{in}, and we get switching with a minimal critical power (defined as the power at which the nonlinear differential phase shift reaches π). At the NOLM output, we select the NOLM output polarization component that is orthogonal to the NOLM input polarization, similarly to the case we described in [13]. As we demonstrated in that paper, when we select at the NOLM output, the polarization component orthogonal to the input polarization state, we obtain a nonlinear transmission dependence that can be used for applications like passive mode locking. When the orthogonal component is selected, the value of the low-power transmission depends of the QWR position, as we can see in Fig. 2. Through the QWR orientation, it is possible to change the transmission behavior from a maximum (75%) to a minimum (0%) at a low input power. In this case, we can see two peaks with different amplitudes (75% and 25%). Note that the maximum low-power transmission can be adjusted easily to between 50% and 100% by adjusting the birefringence of the coupler 1 arms [27].

Figure 3 shows the simulated nonlinear transmission characteristic of the NOLM with the orthogonal output polarization selection for different positions of

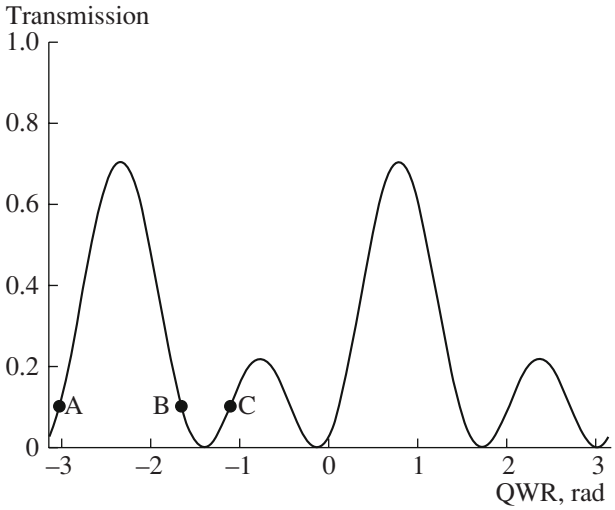

Fig. 2. Theoretical low-power transmission dependence on the QWR plate angle.

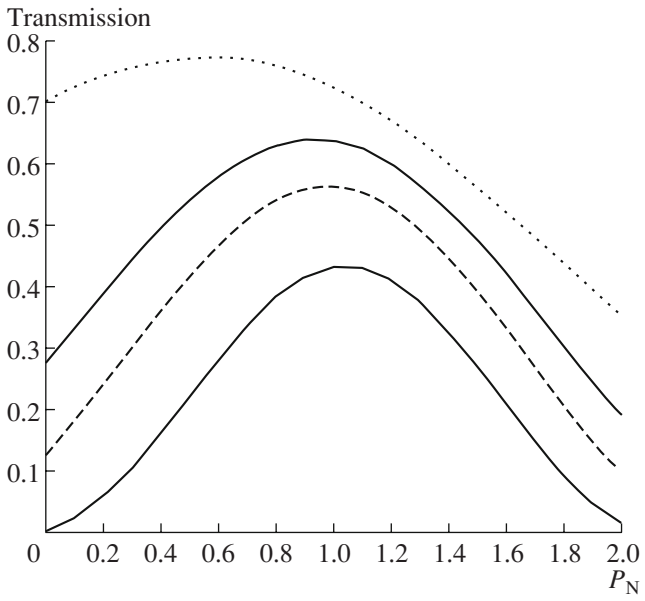

Fig. 3. Nonlinear transmission of the NOLM with an orthogonal output polarization selection functioning of the normalized input power P_N for different positions of the QWR around point A (see Fig. 2).

the QWR on the higher peak of the low-power transmission curve (around point A in Fig. 2). As we can see, when the low-power transmission is too high (say >50%), the nonlinear dependence is mainly decreasing with the power (see dotted curve). This intensity-limiting action, of course, does not favor the mode locking. On the other hand, if the low-power transmission is too small (i.e., close to zero), then nearly all low-power oscillation is absorbed by the NOLM and the laser cannot initiate. At intermediate points like A (see dashed curve), the transmission grows substantially with the power, so that the saturable absorber action is obtained, which allows the mode locking, whereas the low-power transmission is still different from zero making the initial lasing possible. It is, then, understandable that if the intracavity power is sufficient, random positive fluctuations of the power level will be favored through the NOLM and grow leading to the spontaneous pulse formation or the self-starting mode locking.

As we can see in Fig. 2, in terms of the low-power transmission, point B is similar to point A. However, these two points lead to distinct nonlinear dependences. At point A, the nonlinear transmission increases with the input power, whereas, at point B, the nonlinear transmission first decreases to zero before it starts to increase. A similar nonlinear behavior is observed in the second peak in Fig. 2 (point C); however, in this case, the values of the nonlinear transmission are smaller. In this case, the cavity losses are higher for the pulses.

3. EXPERIMENTAL RESULTS

The experimental setup is shown in Fig. 4. The NOLM is formed by a 51/49 coupler 1, whose output ports were fusion spliced with a 220-m loop of low-birefringence, a highly twisted Corning SMF-28 fiber, and a QWR1 in the loop to transform the CCW beam from the circular to the linear polarization. A twist rate of 7 turns/m was imposed to the fiber loop. Prior to the NOLM input, we inserted a QWR2 to circularly polarize the CW beam. Couplers 2 (coupling ratio of 85/15) and 3 (coupling ratio of 99/1) were used to monitor the laser power. We used a circulator to include a fiber-Bragg grating (FBG) as the filtering element in our system. The FBG central wavelength is 1548 nm with 100% reflection. For pumping, we used a 980-nm laser with a 100-mW maximum output power. The pump power was injected into the system through a WDM coupler. The output signal of the NOLM was amplified by a 10-m erbium-doped fiber (with an erbium concentration of 1000 ppm) and passed through a polarization

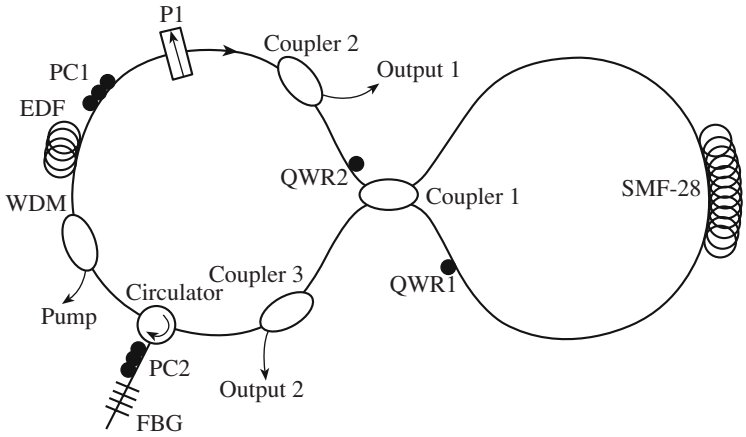

Fig. 4. Schematic of the setup used in the experiment.

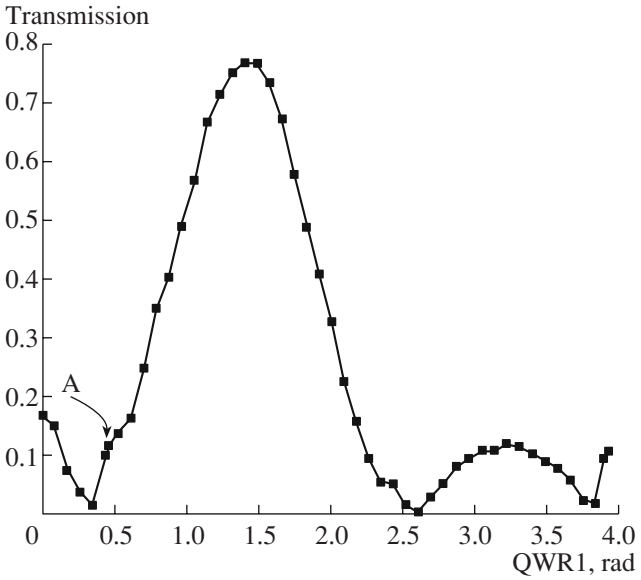

Fig. 5. Experimental low-power transmission dependence on the QWR1 angle when two peaks in a period of π rad have different amplitudes.

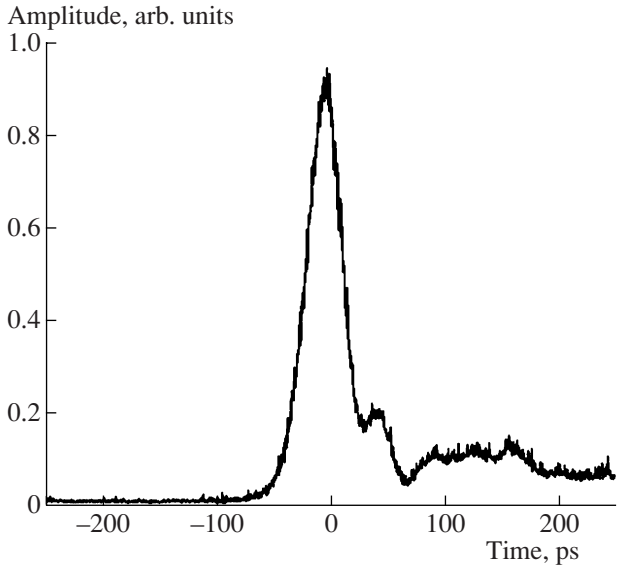

Fig. 6. Pulse waveform monitored with a high-speed photodetector.

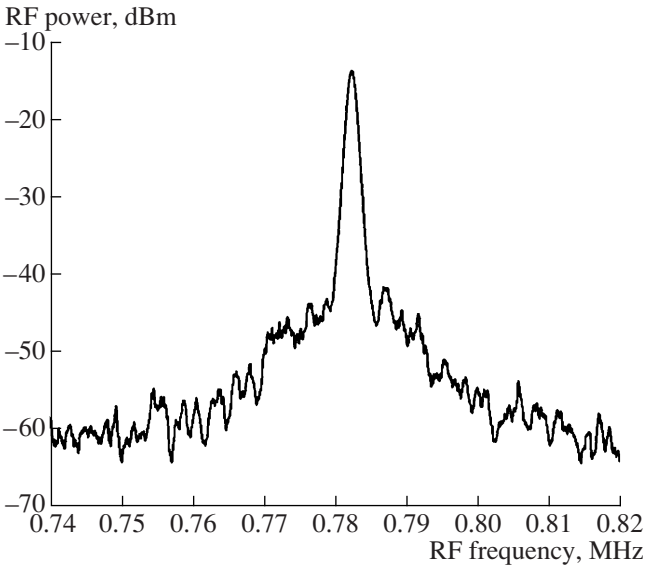

Fig. 7. The pulse train with a 0.787-MHz repetition rate.

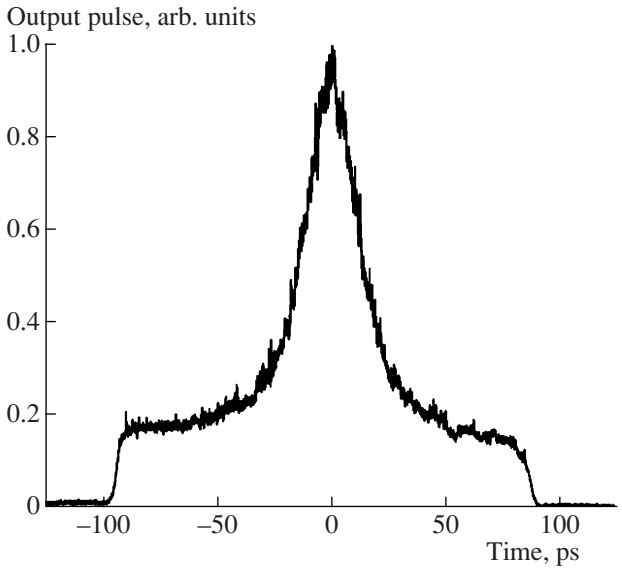

Fig. 8. Autocorrelation trace of the output pulses.

controller (PC1) and the polarizer (P1) to impose the circular polarization at the NOLM input. P1 acts as a polarizer and an optical isolator at the same time, so that light reflected by the NOLM is absorbed. The PC1 and PC2 are adjusted to have a maximal transmission through the P1 using the continuous wave operation. In this case, we are selecting through P1 the NOLM output polarization component that is orthogonal to the NOLM input polarization. Through the QWR1 orientation, it is possible to change the transmission behavior from a maximum (80%) to a minimum (0%) at a low input power, as we can see in Fig. 5. To measure the transmission, we used output 1 as the NOLM input and output 2 as the NOLM output. We believe that the self-starting mode-locked operation requires a low-power transmission amplitude that is different from zero. In Fig. 5, we can see two peaks in a period of π rad, whose amplitudes differ substantially. We can achieve self-starting mode locking when the position of the QWR1 is around point A. As we can see in this figure, the trans-

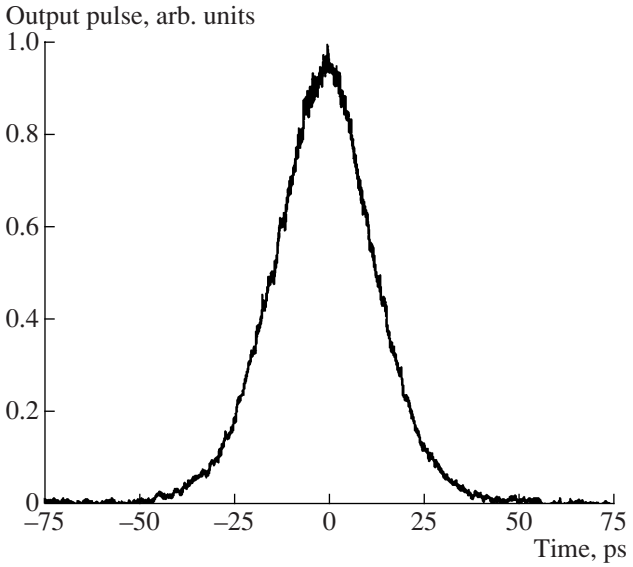

Fig. 9. Autocorrelation trace of the output pulses after the adjustment of the PC2 to eliminate the pedestal of the pulses.

mission at point A is around 11%. At point A, when the pump power is greater than 70 mW, we get self-starting mode-locked pulses.

Figure 6 shows the laser output pulses (at output 1) measured by a fast detector and a sampling oscilloscope when the self-starting first appears with a pump power of around 70 mW. Then, as the pump power is decreased, mode locking is maintained until this power reaches 20 mW. The pulse consists of a 30-ps peak and a long tail. When the pump power drops below 20 mW, the mode locking disappears.

The pulse-train spectrum detected by an RF spectrum analyzer is shown in Fig. 7, where the first harmonic centered at 0.780 MHz is the fundamental frequency of the cavity. The average power at output 1 is 1 mW for a pump power of 70 mW, giving an average power of 5.66 mW entering the NOLM.

Figure 8 shows the autocorrelation function of the output pulses measured by a FR-103XL autocorrelator. The FWHM spectrum bandwidth of the mode-locked signal is $\Delta\lambda = 0.19$ nm. The FWHM of the autocorrelation trace is about 30 ps corresponding to a FWHM pulse duration $\Delta\tau = 21.2$ ps (if a Gaussian profile is assumed) giving $\Delta\nu\Delta\tau = 0.504$, where $\Delta\nu$ is the FWHM of the frequency spectrum. This value is close to the value expected for the transform-limited pulse shapes, indicating that the pulse has a low chirp.

The autocorrelation trace shows the output pulses with a long pedestal monitoring in output 1. We believe that this pedestal is due to the long tail of the pulses shown in Fig. 6. If we adjust the PC2, it is possible to eliminate this pedestal as is shown in Fig. 9. When we do that, however, it is no longer possible to get only one pulse in the cavity; as in this case, a packet of pulses

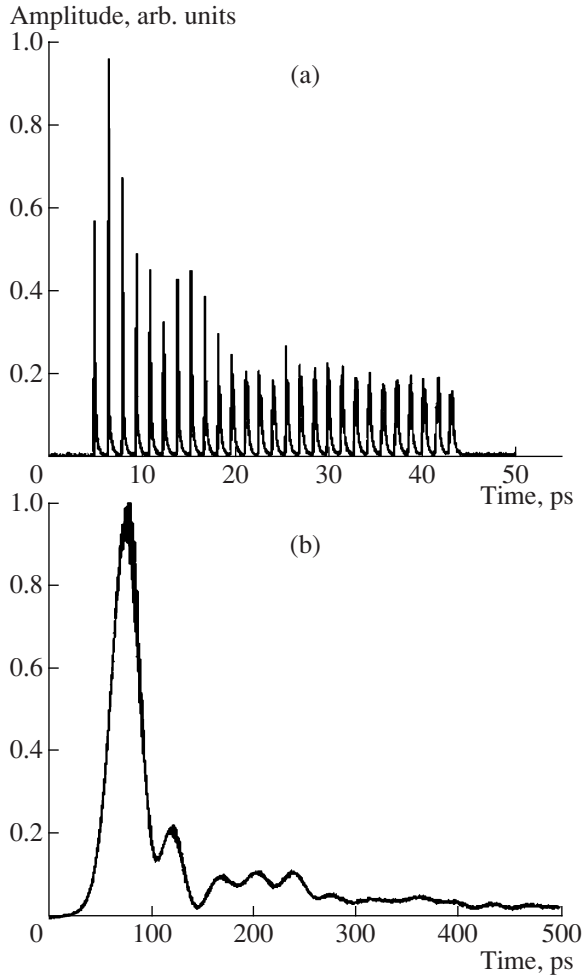

Fig. 10. (a) Laser output pulses measured by a fast detector and a sampling oscilloscope after to adjusting the PC2. (b) Pulse waveform monitored with a high-speed photodetector after adjusting the PC2 to eliminate the long tail of the pulses.

appear, as we can see in Fig. 10a. Monitoring only one pulse, we observe that the long tail is, in this case, almost eliminated (see Fig. 10b).

The present laser has the advantages that the self-starting mode locking can be observed by adjusting only one element—the QWR1 in the NOLM. The adjustment procedure is straightforward; the QWR1 must be around positions A in Fig. 5. After that, we only have to increase the pump power up to 70 mW to get the self-starting mode-locking operation. The stability of the laser is limited by the environmental effects on the fiber, which, over days, required some minor adjustments of the QWR1.

4. CONCLUSIONS

In conclusion, in this work, we demonstrate the operation of a mode-locked F8L based on a symmetrical NOLM with a highly twisted low-birefringence

fiber and a QWR in the loop. With this devise, we can get the self-starting mode locking of the pulses in a special position of the QWR. The pulse-repetition frequency is 0.8 MHz. The FWHM of the autocorrelation function is 30 ps. These pulses have a long pedestal, but we demonstrated that adjusting the PC2 is possible to eliminate this pedestal.

ACKNOWLEDGMENTS

E.K. was supported by CONACYT, grant no. 47169.

REFERENCES

1. A. G. Bulushev, E. M. Dianov, and O. G. Okhotnikov, Opt. Lett. **15**, 968 (1990).
2. I. N. Duling III, Opt. Lett. **16**, 539 (1991).
3. I. N. Duling III and M. L. Dennis, *Compact Sources of Ultrashort Pulses* (Cambridge Univ. Press, Cambridge, 1995).
4. N. H. Seong, D. Y. Kim, and S. P. Veetil, Opt. Commum. **280**, 438 (2007).
5. J. W. Nicholson, S. Ramanchandran, and S. Ghalmi, Opt. Exp. **15**, 6623 (2007).
6. N. J. Doran and D. Wood, Opt. Lett. **13**, 56 (1988).
7. G. P. Agrawal, *Applications of Nonlinear Fiber Optics* (Academic, San Diego, 2001).
8. E. A. Kuzin, B. Ibarra-Escamilla, R. Rojas-Laguna, and J. Sanchez-Mondragon, Opt. Commun. **149**, 73 (1998).
9. E. A. Kuzin, N. Korneev, J. W. Haus, and B. I. Escamilla, J. Opt. Soc. Am. B **18**, 919 (2001).
10. O. Pottiez, E. A. Kuzin, B. Ibarra-Escamilla, et al., Electron. Lett. **40**, 892 (2004).
11. O. Pottiez, E. A. Kuzin, B. Ibarra-Escamilla, and F. Mendez-Martinez, Opt. Commum. **229**, 147 (2004).
12. O. Pottiez, E. A. Kuzin, B. Ibarra-Escamilla, et al., Opt. Express **12**, 3878 (2004).
13. B. Ibarra-Escamilla, E. A. Kuzin, P. Zaca-Morán, et al., Opt. Express **13**, 10760 (2005).
14. T. Tanemura and K. Kikuchi, J. Light Wave Technol. **24**, 4108 (2006).
15. E. A. Kuzin, B. Ibarra-Escamilla, D. E. Garcia-Gomez, and J. W. Haus, Opt. Lett. **26**, 1559 (2001).
16. B. Ibarra-Escamilla, E. A. Kuzin, D. E. Gomez-Garcia, et al., J. Opt. A: Pure Appl. Opt. **5**, S225 (2003).
17. H. A. Haus and E. P. Ippen, Opt. Lett. **16**, 1331 (1991).
18. F. Krausz, T. Brabec, and C. H. Spilmann, Opt. Lett. **16**, 235 (1991).
19. J. Herrmann, Opt. Commun. **98**, 111 (1993).
20. D. J. Richardson, R. I. Laming, D. N. Payne, et al., Electron. Lett. **27**, 542 (1991).
21. H. A. Haus, E. P. Ippen, and K. Tamura, IEEE J. Quantum Electron. **30**, 200 (1994).
22. C. J. Chen, P. K. A. Wai, and C. R. Menyuk, Opt. Lett. **20**, 350 (1995).
23. A. B. Grudinin and S. Gray, J. Opt. Soc. Amer. B **14**, 144 (1997).
24. A. Gordon and B. Fischer, Opt. Lett. **28**, 1326 (2003).
25. A. Gordon, B. Vodonos, V. Smulakovsky, and B. Fischer, Opt. Exp. **11**, 3418 (2003).
26. B. Vodonos, A. Bekker, V. Smulakovsky, et al., Opt. Lett. **30**, 2787 (2005).
27. B. Ibarra-Escamilla, E. A. Kuzin, O. Pottiez, et al., Opt. Commun. **242**, 191 (2004).